第 20 卷 第 3 期
1998 年 5 月

岩 土 工 程 学 报
Chinese Journal of Geotechnical Engineering

Vol.20 No.3
May, 1998

# Pile behaviour in sand through experiments
# 砂土中群桩特性的试验研究

*Peter Onuselogu*(石 磊) *Yin Zongze*(殷宗泽)
(Geotechnical Engineering Research Institute, Hohai University, Nanjing, China, 210098,)

**Abstract** Following the need to study the characteristic responses of piles embedded in sand, a very simple laboratory method was employed through using model piles. The model piles were essentially, perspex pipes instrumented with sensitive strain gauges embedded in their inner surfaces. The load was applied by a manually operated hydraulic jack. The tests were run when the piles were already in position. The results of the experiments were quite typical and demonstrated the soil-pile interaction phenomena. Of interest were the load-sharing characteristics of the pile-shafts and the pile-bases and the contribution of the pile-caps.

**Key words** pile foundation, model test of pile, interaction of pile and soil, pile group efficiencies.

**Peter Onuselogu** Male, born in 1964, Nigeria. In 1990, got master degree(Structure) in university of Lagos. In Hohai University, China, got another master degree(Hydraulic Engineering) in 1991 and doctor degree (Geotechnical Engineering) in 1997.

**文 摘** 为了研究砂土中群桩的受力特性,进行了室内模型桩的试验,模型桩用有机玻璃管做成,内壁贴有敏感的应变片,在桩就位后用一液压千斤顶施加荷载。试验结果相当清楚地反映了桩土的共同作用,其中桩身、桩尖和桩承台上荷载分担规律是很有意义的。

**关键词** 桩基础,桩模型试验,桩土相互作用,群桩效率。
**中图法分类号** TU 411.93

## 1 Introduction

Piles have remained very important structural foundation members because of their special role in transmitting superstructures' loads from zones of weakness to zones of firmness. Due to less machinery requirement for pile installation, their use is often sought when other types of foundation are considered geotechnically, structurally, and financially unsuitable.

The need to investigate driven-pile behaviour in sand in relation to the overburden loads led to the tests carried out in the Geotechnical Engineering Research Institute (GERI) of Hohai University, Nanjing, China.

## 2 Testing program

The existing concrete chamber of dimensions 2100 × 1650 × 1050mm in the GERI laboratory, as shown in figure 1, was filled with river sand passing through sieve of 5mm aperture. This air-dry sand was of loose nature and had the following parameters of Duncan's model:

$$\varphi = 39.7°, c = 0.0\text{kPa}, F = 0.057, R_f = 0.81$$
$$n = 0.61, D = 12.9, K = 665, G = 0.39$$

The model piles were made of transparent pipes of polymethyl metacrylate (PMMA) material otherwise known as perspex. The 30mm external diameter pipes having an annular thickness of 2.5mm were cut to lengths of 750mm

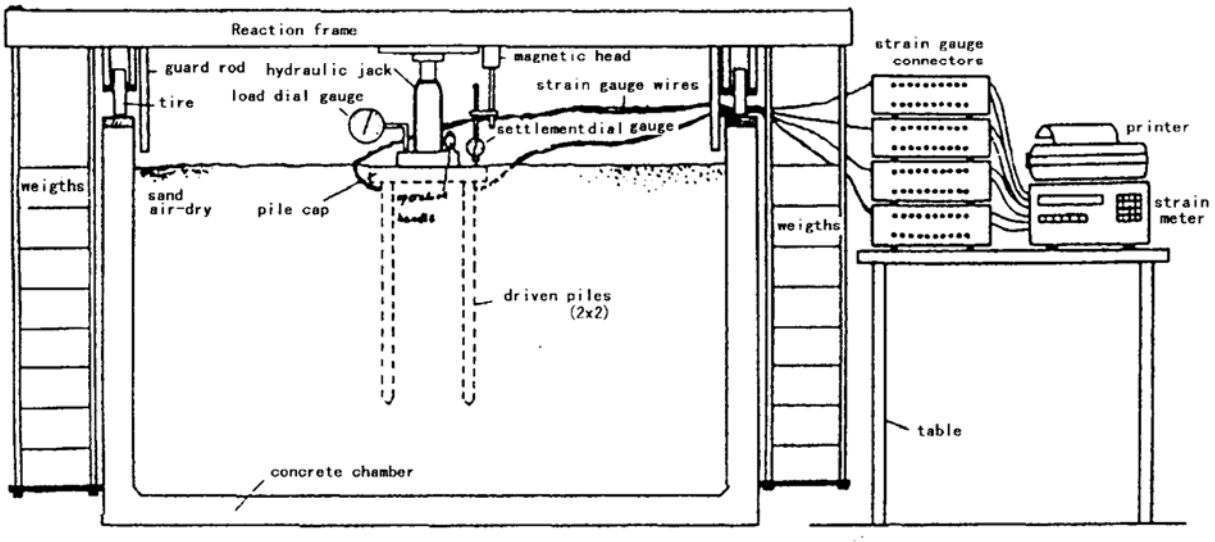


**Fig.1 Schematic presentation of load test apparatus**

Received June 24, 1997.

thereby giving a length-diameter ration (L/D) of 25. To monitor the stress distribution along the piles (when in position), four of the piles were cut longitudinally and strain gauges (8 equidistant bridges with an orthogonal pair making a bridge), were embedded on their inner surfaces. The strain gauge wires of every pipe were passed through a hole drilled on the upper part of the pile and then soldered unto the 20-channel plug. Then , the longitudinal halves were gummed together. At the tip of every pile (whether instrumented or not ) was a wooden solid cone which provided for the end bearing and also prevented sand from entering the pile. The strain gauges were positioned in such a way that the bottom-most bridge (bridge 1) measured approximately the load carried by the pile base, whilst the top-most bridge (bridge 8) approximated the total load carried by pile. See figure 2. The pile-caps were also of wood measuring 25mm in thickness and extending beyond the outer perimeter of a pile or pile group by 1.0D, D being the diameter of pile. The pile caps of single piles were particularly 40 mm square and mainly served to protect the pile head during jacking. On top of the concrete chamber was a steel reaction frame as shown in figure 1.

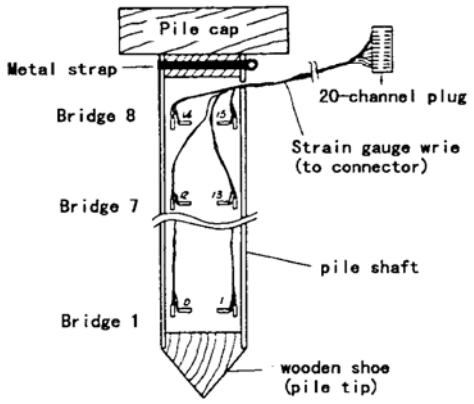


**Fig.2 Instrumented model pile**

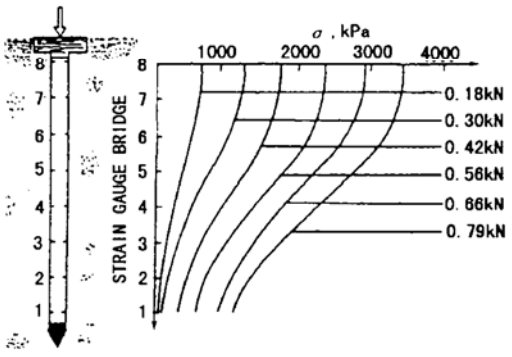


**Fig.3 Stress distribution along single pile**

## 2.1 Pile testing

To run the test , the pile was pushed into the sand as vertically as possible and then jacked down to position until the detachable cap established full contact with the sand. The strain meter was capable of 'cancelling out ' the initial stresses of the driven piles. The load application was made in stages.

# 3 Test results and analysis

## 3.1 Along-pile stress distribution

The distribution of stress along the pile shafts at various loading was measured, see Fig.3 for that of the single piles. It shows the frictional resistance of different sections of the shafts at various load increments. It can be seen that much of the applied load was resisted by the shaft rather than the base during the stages of loading, with the cap virtually carrying no load due its small size. This trend was gradually changed as the base began to take more percentage of the applied load.

This phenomenon was not limited to the isolated piles. The distribution of the average values of the provoked stresses in 2 × 2 pile groups at various spacing and 3 × 3 pile group at 3D centres are shown in figures 3,4 and 5. In these figures, however, the contribution to load-sharing by the pile-caps are more evident, the caps being much bigger and had more contact with soil which was being subjected to lateral compression due to pile displacement of sand particles. This increased the bond between the piles and the pile caps as opposed to the single-pile condition that is considered "relatively loose". Tables 1 through 6 give the summary of test results and also express the load-sharing pattern among the pile-shaft, the pile-base and the pile-cap.

## 3.2 Along-pile load distribution

The instrumentation allowed for the measurement of the actual load each member of a pile group was carrying. The applied load was not equally shared by the piles due to lack of symmetry of the group during load application and also lack of verticality. The distribution of total load ($Q_b + Q_s$) at failure is shown in figure 6.

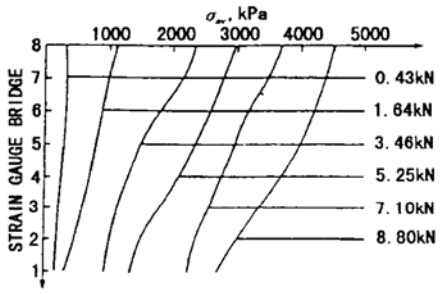


**Fig.4 Stress distribution along 2 × 2 pile group at 4D centres**

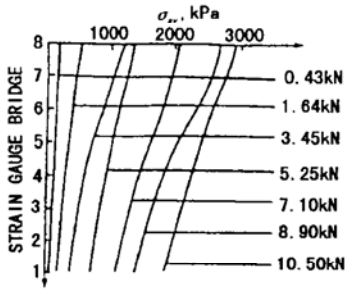


**Fig.5 Stress distribution along 3 × 3 pile group at 3D centres**

**Table 1 Summary of test results and percentage contributions (single pile)**

| total Load(kN) | 0.18 | 0.30 | 0.42 | 0.56 | 0.66 | 0.79 |
|---|---|---|---|---|---|---|
| $Q_b$(kN) | 0.0125 | 0.0231 | 0.0654 | 0.1257 | 0.1959 | 0.2467 |
| $Q_s$(kN) | 0.1367 | 0.2471 | 0.3148 | 0.3743 | 0.4305 | 0.4933 |
| $Q_b + Q_s$(kN) | 0.1492 | 0.2702 | 0.3802 | 0.5000 | 0.6254 | 0.7400 |
| $Q_{cap}$(kN) | 0.0308 | 0.0298 | 0.0398 | 0.0600 | 0.0346 | 0.0500 |
| $Q_b/(Q_b + Q_s)$(%) | 8.37 | 8.55 | 17.20 | 25.14 | 31.27 | 33.34 |
| $Q_s/(Q_b + Q_s + Q_{cap})$(%) | 75.94 | 82.36 | 74.95 | 66.84 | 65.23 | 62.44 |
| $Q_{cap}/(Q_b + Q_s)$(%) | 20.56 | 11.03 | 10.47 | 12.00 | 5.30 | 6.76 |

**Table 2 Summary of test results and percentage contributions (2×2@3D group)**

| Total load(kN) | 0.43 | 10.64 | 3.46 | 5.25 | 6.52 |
|---|---|---|---|---|---|
| $Q_b$(kN) | 0.0974 | 0.2789 | 0.5698 | 1.0428 | 1.3573 |
| $Q_s$(kN) | 0.1804 | 0.6981 | 1.2835 | 1.5932 | 1.7727 |
| $Q_b + Q_s$(kN) | 0.2778 | 0.9770 | 1.8533 | 2.6360 | 3.1300 |
| $Q_{cap}$(kN) | 0.1522 | 0.6630 | 1.6067 | 2.6140 | 3.3900 |
| $Q_b/(Q_b + Q_s)$(%) | 35.06 | 28.55 | 30.75 | 39.56 | 43.36 |
| $Q_s/(Q_b + Q_s + Q_{cap})$(%) | 41.92 | 42.57 | 37.09 | 30.35 | 27.19 |
| $Q_{cap}/(Q_b + Q_s)$(%) | 54.79 | 67.86 | 86.69 | 99.16 | 108.31 |

**Table 3 Summary of test results and percentage contributions (2×2@4D group)**

| Total load(kN) | 0.43 | 1.64 | 3.46 | 5.25 | 7.10 | 8.80 |
|---|---|---|---|---|---|---|
| $Q_b$(kN) | 0.0953 | 0.3371 | 0.8273 | 1.1667 | 1.5984 | 2.3691 |
| $Q_s$(kN) | 0.1887 | 0.6371 | 1.1934 | 1.4149 | 1.5958 | 1.5364 |
| $Q_b + Q_s$(kN) | 0.2840 | 0.9742 | 2.0207 | 2.5816 | 3.1942 | 3.9055 |
| $Q_{cap}$(kN) | 0.1460 | 0.6658 | 1.4393 | 2.6684 | 3.9058 | 4.8945 |
| $Q_b/(Q_b + Q_s)$(%) | 33.56 | 34.60 | 40.94 | 45.19 | 50.04 | 60.66 |
| $Q_s/(Q_b + Q_s + Q_{cap})$(%) | 27.93 | 38.85 | 34.49 | 26.95 | 22.48 | 17.50 |
| $Q_{cap}/(Q_b + Q_s)$(%) | 51.41 | 68.43 | 71.23 | 103.36 | 122.28 | 125.32 |

**Table 4 Summary of test results and percentage contributions(2×2@6D group)**

| Total Load(kN) | 0.43 | 1.64 | 3.46 | 5.25 | 7.10 | 8.00 |
|---|---|---|---|---|---|---|
| $Q_b$(kN) | 0.1026 | 0.2873 | 0.5637 | 1.0571 | 1.5541 | 1.7762 |
| $Q_s$(kN) | 0.2149 | 0.7424 | 1.3587 | 1.6019 | 1.8129 | 1.9016 |
| $Q_b + Q_s$(kN) | 0.3175 | 1.0297 | 1.9224 | 2.6590 | 3.3670 | 3.6778 |
| $Q_{cap}$(kN) | 0.1125 | 0.6103 | 1.5376 | 2.5610 | 3.7330 | 4.3222 |
| $Q_b/(Q_b + Q_s)$(%) | 32.31 | 27.90 | 29.32 | 39.76 | 46.17 | 48.30 |
| $Q_s/(Q_b + Q_s + Q_{cap})$(%) | 50.00 | 45.27 | 39.27 | 30.51 | 25.53 | 23.77 |
| $Q_{cap}/(Q_b + Q_s)$(%) | 35.43 | 59.27 | 79.98 | 97.44 | 110.87 | 117.52 |

**Table 5 Summary of test results and percentage contributions(3×3@3D group)**

| Total Load(kN) | 0.43 | 1.64 | 3.46 | 5.25 | 7.10 | 8.90 | 10.50 |
|---|---|---|---|---|---|---|---|
| $Q_b$(kN) | 0.1190 | 0.3330 | 0.9515 | 1.4094 | 1.9341 | 2.7642 | 3.6703 |
| $Q_s$(kN) | 0.2015 | 0.6748 | 1.4135 | 1.7569 | 2.0900 | 2.4948 | 1.9820 |
| $Q_b + Q_s$(kN) | 0.3205 | 1.0078 | 2.3650 | 3.1663 | 4.0241 | 5.2602 | 5.6523 |
| $Q_{cap}$(kN) | 0.1095 | 0.6322 | 1.0950 | 2.0837 | 3.0759 | 3.6398 | 4.8477 |
| $Q_b/(Q_b + Q_s)$(%) | 37.13 | 33.04 | 40.23 | 44.51 | 48.06 | 52.55 | 64.93 |
| $Q_s/(Q_b + Q_s + Q_{cap})$(%) | 48.86 | 41.15 | 40.85 | 33.46 | 29.44 | 29.03 | 18.86 |
| $Q_{cap}/(Q_b + Q_s + Q_{cap})$(%) | 34.17 | 62.73 | 46.30 | 65.80 | 76.44 | 69.20 | 855.77 |

**Table 6 Group load-sharing conditions at failure**

| Pile Group | Average Load(kN) | Max. tage greater than Ave.(%) | Min. tage less than Ave.(%) | Max. carrying difference(kN) |
|---|---|---|---|---|
| 2×2@3D | 0.7825 | 2.63 | 2.72 | 0.0419 |
| 2×2@4D | 0.9764 | 3.46 | 2.91 | 0.0622 |
| 2×2@6D | 0.9195 | 1.92 | 3.20 | 0.0471 |
| 3×3@3D* | 0.6280 | 61.38 | 10.38 | 0.4459 |

* Only four piles were instrumented, average values computed based on the incorrect assumption of load distribution symmetry.

**Table 7 Group efficiencies**

| Pile | load per pile(kN) | | | | efficiencies | | | |
|---|---|---|---|---|---|---|---|---|
| | Point load | Skin load | Total load | Total+ * | Point | Skin | Total | Total+ * |
| 1×1 | 0.2467 | 0.4933 | 0.7400 | 0.7900 | 1.00 | 1.00 | 1.00 | 1.00 |
| 1×1 | 0.2510 | 0.5050 | 0.7560 | 0.7900 | 1.02 | 1.02 | 1.02 | 1.00 |
| 2×2@3D | 0.3393 | 0.4432 | 0.7825 | 1.6300 | 1.36 | 0.90 | 1.06 | 2.06 |
| 2×2@4D | 0.5923 | 0.3841 | 0.9764 | 2.2000 | 2.40 | 0.78 | 1.32 | 2.78 |
| 2×2@6D | 0.4440 | 0.4754 | 0.9194 | 1.7319 | 1.80 | 0.96 | 1.24 | 2.19 |
| 3×3@3D | 0.4078 | 0.2202 | 0.6280 | 1.1667 | 1.65 | 0.45 | 0.85 | 1.48 |

* Total+ means Total plus cap

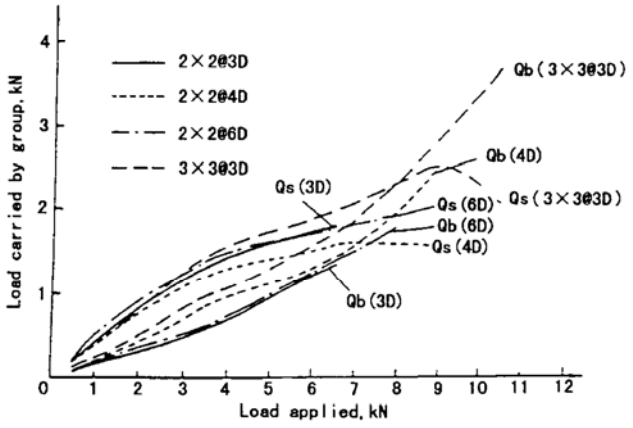


**Fig.6 Distribution of base and shaft loads(pile group)**

For the 2×2@3D group, the interaction between the base and shaft seems very similar to that of single pile as both shaft load $Q_s$(3D) and the base load $Q_b$(3D) have nearly the same gradient. The next group, 2×2@4D, had a remarkable base – shaft interaction as the rising arm of the shaft load curve $Q_s$(4D) suddenly fell to compensate for the simultaneous rise in the amount of load carried by base as indicated by curve $Q_b$(4D). The group at 6D centres interacted very similarly to that at 3D centres for their interaction curves almost coincide. The last group, 3×3@3D, also had a remarkable base – shaft interaction with the base receiving the 'lost' load by shaft when it started to fail in settlement. Curve $Q_s$(3×3@3D) shows that in settlement-induced failure, the shaft capacity at failure of a pile may be less than the shaft load which previously carried (before failure). This is also true for $Q_s$(4D) considering the 2×2 pile group.

## 3.3 Pile group efficiencies

The efficiencies of all the piles tested were as shown in table 7. Of interest is the sub-unity efficiencies of shaft capacities of pile groups with the point efficiencies always greater than 1. This shows that at failure , and the shaft percentage contribution gets reduced mainly because settlement weakens and breaks the frictional bond between the shaft and the surrounding soil particles.

The pile-cap contribution is very evident from table 7. The pile system had much increased capacity due to the caps. The variation of efficiency due to pile spacing is equally shown in the table and suggests that the 2×2 pile group had their optimum spacing at a value just greater than 4D. This is true for both 'Total' and 'Total + cap' and has been represented graphically in figure 7.

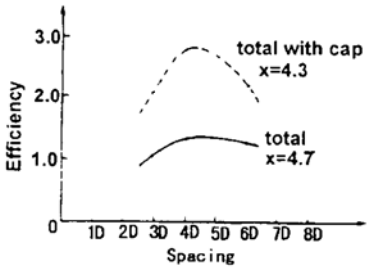


**Fig.7 2×2 pile group efficiencies**

## 3.4 Settlement

This is proved to be a major limiting factor to group capacity for it leads to group failure even at low-stress values in the group members. Notably, the total load per pile of the 3×3@3D group was only 0.6280kgf (as opposed to 0.74kN of the single pile and 0.9764kN of the 2×2@4D group for that matter). It can be seen from figure 8 that the settlement of an isolated pile which became asymptotic after 5mm at 0.79kN. The settlement of pile groups were much larger with 2×2@3D group signalling off after 12mm and 2×2@4D failing after 13.2mm. The group, 2

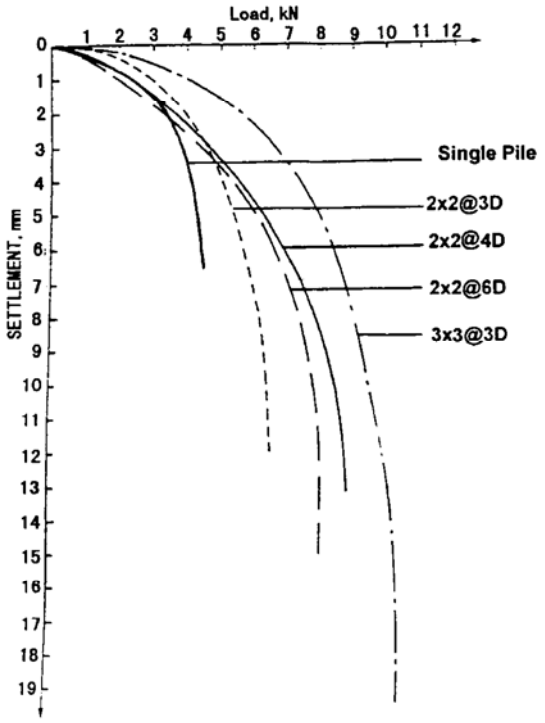


**Fig.8 Load settlement curve of piles**

× 2@6D recorded a higher settlement than its predecessors while the 3 × 3@3D group had the largest vertical displacement.

## 4 Conclusion

The following points can be deduced from the analysis of the test results.

(1) For driven piles in sand environment, the friction contribution to load sharing, which is usually significant, can be more in single piles than in pile groups.

(2) The high-friction component of the capacity of driven single piles reduces the group friction efficiency even though the sand enclosed within the group is laterally compressed by virtue of sand particle displacement during driving.

(3) The interaction between pile shaft and pile base and possibly pile cap leads to load redistribution. Particularly, in settlement-induced failures, which is often the case with pile groups, the value of the shaft load may start reducing at some point. This phenomenon may lead to catastrophic collapse of structures on piles if the redistributory compensation from pile bases and pile caps is not large enough.

(4) The closer the piles in a group, the less-spread and hence the less-intense the effect of the pressure becomes on distant soil particles. Settlement is provoked by both the size of the pile's zone of influence and the pressure intensity within the zone of influence.

## References

1 Chow Y K. Analysis of vertically loaded pile groups. Int J of Num and Analyt Method in Geothch. 1986. **10**: 59 ~ 72.

2 Lee M W, Lee W J, Paik S W and Yoon S J. Simple pile loading Test technique – The principle and applications. Proc 9th Asian Regional Conference on Soil Mechanics and Foundation. 1991.

3 Madhav M R and Poorooshasb H B. A new method for estimating pile group efficiency. Indian Geotechnical Journal. 1993. **23**(3): 314 ~ 329.

4 Poulus H G. Prediction of axial behaviour of piles. Predicted and Observed axial behavior of piles. ASCE Geotechnical Special publication No 23. 1989: 83 ~ 95.